Analysis of Collision Induced Dissociation of $Na_2{}^+$ Molecular Ions

J. C. Brenot,* H. Dunet, J. A. Fayeton, M. Barat, and M. Winter
Laboratoire des Collisions Atomiques et Moléculaires (URA281), Université Paris-Sud, 91405 Orsay Cedex, France

(Received 12 April 1996)

A full analysis of the collision induced dissociation of a diatomic molecular ion is presented for the first time. The experiment is essentially based on the simultaneous measurement of the momenta of the two fragments. This technique applied to the collision of $Na_2{}^+$ with a helium target reveals, at keV collision energies, the competition between two dissociation mechanisms: an impulsive mechanism when the target hits one Na^+ core in a close encounter and an electronic mechanism when dissociation occurs after excitation of repulsive or weakly bound states. [S0031-9007(96)00952-0]

PACS numbers: 34.50.Pi, 34.50.Lf

Collision induced dissociation (CID) of diatomic molecules is an example of a three body interaction which is not yet fully understood. Back in the sixties, the study of CID of $H_2{}^+$ molecules was initially motivated by the need to produce fast H atoms for heating plasma of interest for thermonuclear fusion. Then, during the seventies, an intense activity developed when it was demonstrated that accurate measurements of momentum distributions of dissociation fragments produced in fast collisions were a powerful tool to access the spectroscopy of molecular ions with meV accuracy [1]. Termed "translational spectroscopy," this technique allows for such an accuracy, owing to the magnification introduced by the laboratory–to–center-of-mass (CM) transformation of the momentum distribution of the fragments. Our knowledge of this field is well summarized in the review of Los and Govers [2]. In the keV energy range and for the investigated systems, the collision time is much shorter than the dissociation time of the molecule, allowing approximations in terms of "two step" mechanisms. In the first step, the molecule is excited into an unstable state. In the second step, dissociation occurs far from the perturbing partner of the collision. As first proposed by Durup [3], two classes of mechanisms have been considered, depending on the *first step* of the collision.

(i) A close encounter between one atomic core of the molecule and the target atom, the other atomic core remaining spectator, leads to a large stretching of the molecule resulting in vibrational excitation, increasing with the scattering angle [4]. Such a mechanism, hereafter referred to as the *impulse mechanism* (IM), has been identified by measuring the energy losses undergone by a molecular projectile as a function of the scattering angle [5]. In such a collision induced vibrational excitation, the molecule dissociates when the energy transfer is large enough. Although often invoked, this dissociation mechanism has never been directly observed. Notice that such a binary impulse mechanism has already been invoked as an initial step for reactive collision processes at moderate energy [6].

(ii) In a more distant collision, the target may primarily interact with the electron cloud of the molecule which can be electronically excited into a dissociative state. In fact, in most of the investigated cases, this excitation results from an electron capture by the molecular ion at large impact parameter to a dissociative [7] or predissociative state [8]. Such processes, referred to as the *electronic mechanism* (EM), somewhat analogous to photodissociation, do not require, in contrast to mechanism IM, a large deflection of the CM of the molecule. Thus, assuming a negligible scattering angle, a measurement in coincidence of the two fragments scattered in the forward direction allows for a full determination of the momentum distribution by only measuring the difference of arrival times and the distance of the two fragments [9].

The new type of experiment reported in this Letter allows for the first complete study of a CID process without any assumption on the CM deflection, an analysis which requires a full determination of the *momenta of both fragments.* For this purpose, the velocity vectors of the two fragments are determined by a simultaneous measurement of their times of flight and of their impact locations onto two position sensitive detectors. Such a complete 3D momentum analysis gives access to energies as well as polar and azimuthal angular distributions of the dissociation products which, in turn, gives some insight into the role played by the relative orientation of the collision plane and dissociation plane. With this technique, we were able for the first time to show evidence of the *impulse mechanism* occurring in violent collisions and its competition with the *electronic* dissociation. These results were obtained for $Na_2{}^+$ molecular ions colliding with a helium target at 1 keV collision energy and dissociating into Na^+ and Na fragments. The other channels will not be considered here.

In the present experiment, Na_2 dimers are formed in an adiabatic expansion from an oven heated at 750° C. The beam is then ionized by 30 eV electrons. After acceleration at 1 keV energy and focusing, the beam is mass selected with a Wien filter and chopped at a frequency of 1 MHz. The $Na_2{}^+$ chopped beam is crossed at 90° with a cold helium target beam issued from a supersonic expansion. Use of a cold target is necessary to minimize the effect of the thermal target motion on the velocity spread of the scattered beam. The collision volume is located at the focus point of a 30° parallel plate electrostatic analyzer, allowing for separation of neutral and charged fragments. It is also used to mass select the ionic fragment. The Na^+ ions are received on a two dimension position sensitive detector (PSD) with a 0.1 mm resolution. The neutral fragments fly in straight line, through the electrostatic analyzer and through a fine mesh grid stretched on the outer plate, and finally are detected with a second PSD. Flight times of both fragments are measured using a multihit multistop time digitizer having a 0.5 ns resolution and triggered by the beam chopper. From the determination of the times of flight (TOF) and of the locations of the two coincident events, one is able to determine the velocity vectors of both fragments and, hence, to *fully reconstruct the kinematics* of the collision process provided that dissociation occurs in the collision volume (15 ns transit time). The energy spread of the chopped incident beam measured by the electrostatic analyzer is less than 2 eV. The accuracy of the velocity measurements is primarily limited by the time width of the beam (10 ns for a total TOF of 5 μS) and the spatial width of the beam (0.5 mm for a fly length of 350 mm), resulting in a 0.15 km/s accuracy compared to typical fragment velocities of 65 km/s (5.2 km/s CM). Actually, the precision on the relative velocity of fragments is by far better since its components are determined from the differences of laboratory data accurately obtained from coincident particles. The detailed description of the experimental procedure will be given elsewhere.

The velocity diagram of Fig. 1 shows, in the CM frame, the geometric parameters relevant for the CID process. The collision plane C and the dissociation plane D are particularized, leading to the choice of the three angles Φ, α, and χ to characterize the collision process. The scattering angle χ of He is also that of the CM of the two fragments, a parameter which will be used as a measure of the collision strength. Φ is the angle between the dissociation plane and the collision plane, whereas α measures the tilting of the relative dissociation velocity vector $\mathbf{V}_{Na^+} - \mathbf{V}_{Na}$ with respect to the final He recoil velocity vector.

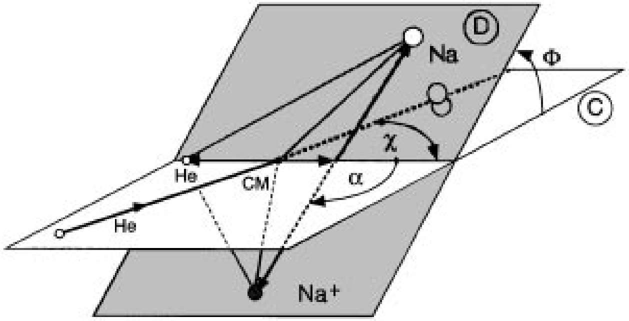

FIG. 1. CM velocity diagram for the $Na_2{}^+$ + He collision induced dissociation.

In a multiparametric experiment, one has to look for correlation in data using the most significant parameters. A first type of such correlation is provided by the contour map of the dissociation events (Fig. 2) in the (E_{rel}, χ) coordinates, where E_{rel} stands for the relative kinetic energy of the two fragments. Clearly, three peaks show up. Let us first discuss structure I. Such a process appears at large scattering angles. It should be noticed that the tail of peak 1 indicates that E_{rel} increases with increasing scattering angle χ. This behavior suggests that structure I is due to the *impulse mechanism* in which one of the Na^+ atomic core hits the He target resulting in a rovibrational excitation of $Na_2{}^+$ in the ${}^2\Sigma_g$ $3s$ ground state (Fig. 3) above the dissociation limit. In this model, the relative energy of the fragments is given by the difference between the kinetic energy ΔE transferred during a Na-He elastic collision and the energy E_D required to dissociate $Na_2{}^+$ (Fig. 3). E_D is given by $E_{D0} - E_{int}$ with $E_{D0} = 0.96$ eV and E_{int} being the binding energy of $Na_2{}^+$ and the internal (rovibrational) energy of incident $Na_2{}^+$, respectively (Fig. 3). The corresponding $E_{rel}(\chi)$ curves are reported in Fig. 2 for the two limiting cases: $E_{int} = 0$ eV for $Na_2{}^+$ in the vibrational ground state and $E_{int} = E_D$. The similar χ dependence of the curves and of the experimental contour plots supports our interpretation. As a result, one can estimate the initial $Na_2{}^+$ internal energy distribution to be around 0.2 eV.

The present vectorial analysis actually provides more insight into the dissociation mechanism, as, e.g., the angle Φ between the collision plane and the dissociation

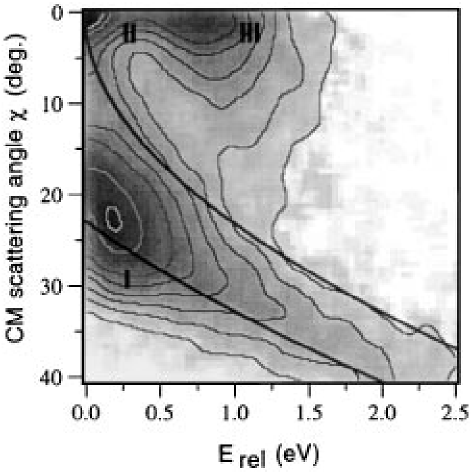

FIG. 2. Contour map of the intensity for the $Na_2{}^+ + He \rightarrow Na^+ + Na + He$ dissociation as a function of the relative kinetic energy of the fragments E_{rel} and the CM scattering angle χ showing the three structures discussed in the text. All contour levels show a logarithmic intensity scale with a factor of 1.6 between each contour. The two solid curves represent $E_{rel}(\chi)$ given by the impulse model for the two limiting values of the initial internal energy of $Na_2{}^+$: $E_{int} = 0$ (bottom curve) and 0.96 eV.

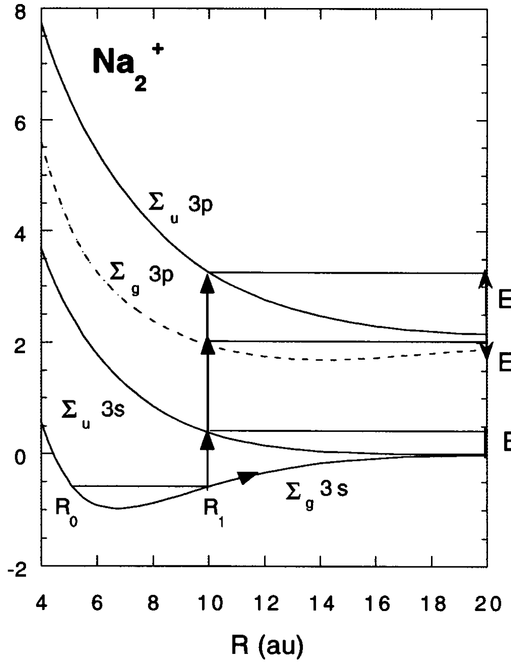

FIG. 3. Potential energy curves of the lowest Σ states of $Na_2{}^+$ taken from Ref. [10]. E_{rel} represents the relative kinetic energies of the two fragments.

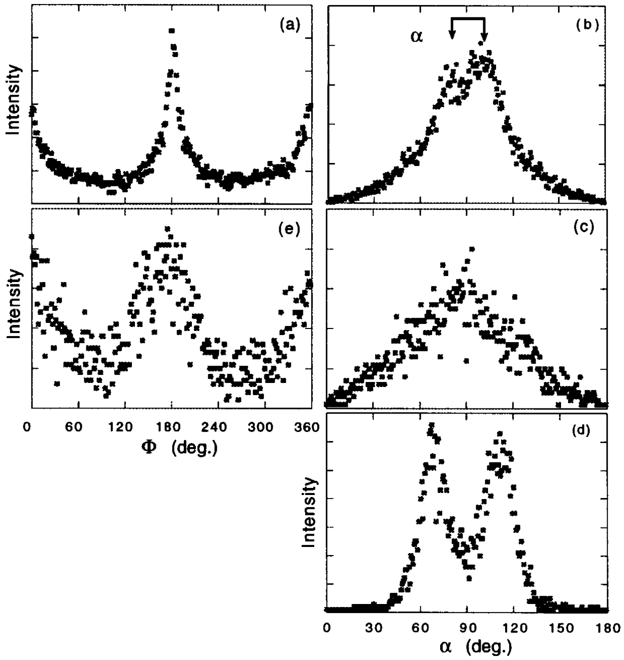

FIG. 4. (a) Distribution as a function of Φ for process I. (b) Distribution as a function of α for process I; the two arrows indicate the α values predicted by the impulse model for scattering angle $\chi = 20°$ and $\Phi = 0°, 180°$. (c), (d) Distribution as a function of α for processes II and III, respectively. (e) Distribution as a function of Φ for processes II and III.

plane. In the impulse mechanism, it is assumed that a Na core is first hit by the He target atom, and then the momentum transfer is transformed into internal energy of $Na_2{}^+$. In this model, the Na-He scattering defines the collision plane (Fig. 1). If the dissociation process is assumed to occur far from the He atom, one may neglect the residual interaction with the third body. Within this assumption, the dissociation should also take place around the collision plane ($\Phi = 0°$ and $180°$). The determination of the angle Φ thus provides an additional test of the validity of the model. This can be done by "filtering" the data corresponding to structure I, i.e., by selecting the events having $\chi > 10°$. Such an analysis indeed shows [Fig. 4(a)] a large propensity for a dissociation occurring *in* the collision plane in agreement with the model.

The dependence of the process with the angle α provides another test of the model. The impulse mechanism implies that the dissociation axis should be aligned with the momentum transfer given by the elastic collision between the Na core and the He target. This imposes a simple relationship between α and the scattering angle χ. Figure 4(b) shows the α dependence of the experimental intensity integrated in the $15° < \chi < 25°$ angular range for which the process dominates. It is readily seen that the two maxima of the distributions agree well with the α value predicted by the model for the average value $\chi = 20°$ and $\Phi = 0°, 180°$.

The other structures (II and III) in Fig. 2 correspond to processes characterized by relative energies around $E_{\text{rel}} = 0$ and 0.7 eV, respectively. These structures appear in a restricted angular range $\chi < 5°$, and their energy profiles are almost independent of the scattering angle. Such processes occurring in the forward direction are assumed to be due to the electronic mechanism EM, involving electronic transitions toward weakly bound (structure II) or repulsive (structure III) excited states of $Na_2{}^+$, depending on the E_{rel} values. Actually, comparison between these energy losses and that of process I allows for the identification of the relevant excited states (Fig. 3). The energy loss profile corresponding to structure II is found to be centered around 2.5 eV. This process, associated with a very low relative energy of the fragments E_{rel}, is assigned to the dissociation of the weakly bound ${}^2\Sigma_g^+\ 3p$ or ${}^2\Pi_u\ 3p$ states for which the energy loss corresponds to the Na($3s$)-Na($3p$) excitation energy. The corresponding α dependence [Fig. 4(c)] shows a preferential dissociation for $Na_2{}^+$ oriented at 90° with respect to the incident beam. On the other hand, the α dependence of structure III [Fig. 4(d)] reveals two peaks around $\alpha = 70°$ and $\alpha = 110°$ which correspond to dissociation of different electronic states. Filtering the data with two bands centered onto these two α angles reveals that the two groups of data are indeed associated with two different energy losses. A first process corresponding to the smallest angle $\alpha = 70°$ has an energy loss < 1 eV and can be ascribed to the dissociation of the lowest repulsive state ($^2\Sigma_u^+$ 3s). Notice that the corresponding relative energy of the fragments $E_{\text{rel}} = 0.7$ eV (Fig. 1) is consistent with an initial internal energy $E_{\text{int}} < 0.2$ eV deduced from the analysis of process I and assuming a vertical transition $^2\Sigma_g^+ \rightarrow {}^2\Sigma_u^+$ at R_1 (Fig. 3). Finally, the last structure for $\alpha = 110°$ is associated with the largest energy loss of 3 to 4 eV and would correspond to the dissociation of higher repulsive states such as $^2\Sigma_u^+$ 3p or $^2\Pi_g^+$ 3p states, the identification of which is limited by the energy resolution of the measurements. The Φ angular distribution for the sum of all electronic processes also exhibits a preferential "in-plane" dissociation [Fig. 4(e)], although not as marked as for process I. This may be due to the difficulty to characterize the collision plane for small scattering angles χ.

The relative importance of the various dissociation processes has been estimated after integration of the multiply differential data as being about $(70 \pm 10)\%$ for the impulse process and about 10% for each of the three electronic processes. Notice that most of the previous CID experiments were focused on the spectroscopy of the predissociating molecular states relevant of the EM mechanism [2] and did not pay much attention to the quantitative importance of the relative contribution of IM. The present results suggest new measurements of the relative contributions of both types of CID processes.

In conclusion, using a new multiparametric coincidence technique, providing a 3D angular investigation of a molecular fragmentation, a first complete analysis of the dynamics of the collision induced dissociation of a diatomic molecule has been obtained. Such an analysis which does not neglect [2] the deflection of the CM of $\text{Na}_2{}^+$ reveals the competition between two mechanisms: a rovibrational dissociation when the target atom suffers a rather violent collision with one Na core, and a softer dissociation following an electronic excitation. It is noteworthy that the impulse mechanism gives the largest contribution, although requiring a small impact parameter. This indicates a much larger transition probability for this mechanism as compared to the electronic dissociation. The angular analysis shows a large dominance of dissociation in the collision plane for both cases. The most promising development of this technique is provided by the investigation of the collision induced dissociation of small metallic clusters. For example, preliminary results show that $\text{Na}_3{}^+$ dissociates only following the impulse mechanism in the $\text{Na}_2{}^+ + \text{Na}$ channel.

We wish to thank the Laboratoire Aimé Cotton for providing us with the sodium cluster source. One of us (M. W.) acknowledges support from the European Community Research funds for a Post Doc grant. This work was supported by the EU through a "Human Capital and Mobility" Network "Collision Induced Cluster Dynamics."

---

*Electronic address: brenot@lcam.u-psud.fr

[1] J. Schopman, P. G. Fournier, and J. Los, Physica (Amsterdam) **63**, 518 (1973).

[2] J. Los and T. R. Govers, in *Collision-Induced Dissociation of Diatomic Ions*, Collision Spectroscopy edited by R. G. Cooks (Plenum Press, New York and London, 1978), pp. 289–353.

[3] J. Durup, in *Recent Developments in Mass Spectrometry*, edited by K. Ogata and T. Hayakawa (University of Tokyo Press, Tokyo, 1970), p. 921.

[4] T. A. Green, Phys. Rev. A **1**, 1416 (1970).

[5] J. Fayeton, A. Pernot, P. Fournier, and M. Barat, J. Phys. (Paris) **32**, 743–750 (1971).

[6] D. R. Bates, C. J. Cook, and J. F. Smith, Proc. Phys. Soc. London **83**, 49 (1964); Ch. Ottinger and S. Zimmermann, Chem. Phys. **53**, 293 (1980).

[7] See, e.g., D. P. de Bruijn, J. Neuteboom, V. Sidis, and J. Los, Chem. Phys. **85**, 215 (1984); A. B. van der Kamp, R. S. Hiemstra, W. J. van der Zande, R. Fink, and M. Jungen, J. Chem. Phys. **99**, 7487 (1993).

[8] P. Fournier, C. A. van de Runstraat, T. R. Govers, J. Schopman, F. J. de Heer, and J. Los, Chem. Phys. Lett. **9**, 426 (1971).

[9] D. P. de Bruijn and J. Los, Rev. Sci. Instrum. **53**, 1020 (1981).

[10] A. Henriet, O. Dulieu, and F. Masnou-Seeuws, Z. Phys. D **18**, 287 (1991).